Hindawi
International Journal of Polymer Science
Volume 2021, Article ID 6671681, 9 pages
https://doi.org/10.1155/2021/6671681

*Research Article*

# Electrical Treeing and Partial Discharge Characteristics of Epoxy/Silica Nanocomposite under Alternating Current

**Jae-Jun Park**

*Department of Electrical and Electronic Engineering, Joongbu University, 305 Dongheon-ro, Deogyang-gu, Goyang-si, Gyeonggi-do 10279, Republic of Korea*

Correspondence should be addressed to Jae-Jun Park; jjpark@joongbu.ac.kr

Received 12 October 2020; Revised 27 January 2021; Accepted 5 February 2021; Published 24 February 2021

Academic Editor: Marta Fernández García



The hydrophilic surface of fumed nanosilica was modified to a hydrophobic surface by treating it with a trimethyl silane coupling agent, and epoxy nanocomposites were prepared by mixing the modified nanosilica (0 phr, 1 phr, 3 phr, 5 phr, and 7 phr) in an epoxy matrix, where the unit phr means the parts per one hundred grams of epoxy base resin. To apply the nanocomposites to heavy electrical equipment, the effects of the modified nanosilica on the long-term treeing phenomena and the partial discharge (PD) resistance were studied under high voltage alternating current (HVAC) conditions. The bonding of trimethyl silane on the nanosilica surface was confirmed by the appearance of new peaks for the $CH_2$ and $CH_3$ groups in Fourier-transform infrared spectroscopy analysis. To observe the even dispersion of the modified nanosilica particles in the epoxy matrix, a transmission electron microscope was employed, and it was found that 1 phr of the modified nanosilica was uniformly dispersed; however, as the nanosilica content was increased, its aggregation became somewhat severe. The longest HVAC treeing breakdown time was found in an epoxy nanocomposite with 1 phr of alkyl-modified nanosilica, and the time was 17,412 min, which was 143.9 times longer than the 121 min required for a neat epoxy system. In a nanocomposite with 5 phr of modified nanosilica, PD resistance was found to be 12.5 times higher than that of the neat epoxy system.

## 1. Introduction

Epoxy resins are well known as materials used in heavy electrical equipment, because they have excellent electrical insulating properties together with good mechanical and thermal properties [7, 10, 11]. Epoxy resins are generally used in the form of microcomposites or nanocomposites. Representative microsized and nanosized fillers include silica, alumina, clay, and mica, which can be used independently or in combination depending on the application of the composites [12–14]. These fillers in an epoxy matrix retard the treeing initiation process and block the propagation process effectively, and as such, well-dispersed fillers can sufficiently improve the treeing breakdown strength [7]. In general, 50-65 wt% of microsized fillers are incorporated into epoxy resins in microcomposites, and 3-5 wt% of nanosized fillers are mixed into epoxy resins in nanocomposites [7, 15, 16]. However, in order to achieve a good electrical insulation property, the surface of the hydrophilic fillers should be modified to have hydrophobic characteristics, because the epoxy matrix has hydrophobic characteristics. Surface modification of a filler is generally obtained by using coupling agents in order to both increase the affinity between the epoxy matrix and the inorganic filler and disperse the filler uniformly in the matrix [17, 18]. The molecular structure of a coupling agent has an inorganic reactive group on one side and an organic reactive group on the other side. The former reacts with the microsized or nanosized inorganic filler, while the latter bonds to the epoxy group or curing agent in the epoxy matrix. Therefore, the inorganic filler can easily be dispersed in the epoxy matrix without aggregation. Partial discharge (PD) resistance must also be studied in order to develop a new polymeric insulation material. When PD is applied to the insulating materials for high voltage equipment, it results in the formation of electrical treeing and in the degradation of the insulators [19, 20].

To make silica nanoparticles which are able to retard the treeing initiation and block the treeing propagation, for this

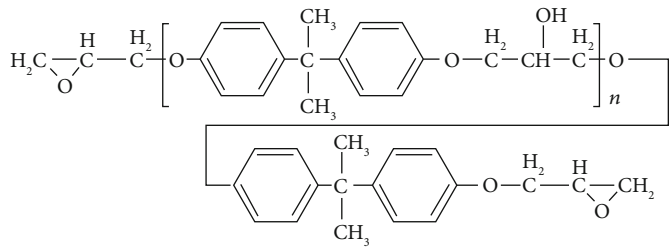

Diglycidyl ether of bisphenol A (DGEBA, YD-128)

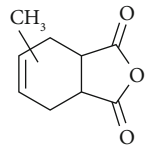

Methyl tetrahydrophthalic anhydride (Me-THPA)

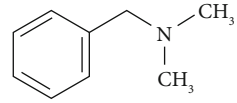

Benzyl dimethylamine (BDMA)

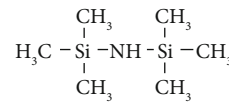

1,1,1,3,3,3-Hexamethyl disilazane (HMDA)

Figure 1: Chemical structure of reagents.

paper, the surface of hydrophilic nanosilica was modified with a trimethyl silane coupling agent and the surface-modified nanosilica was mixed with an epoxy matrix, and the electrical treeing and partial discharge characteristics were studied.

## 2. Experimental Work

*2.1. Materials.* Diglycidyl ether of bisphenol A (DGEBA) type epoxy resin whose trade name was YD 128 (Kukdo Chem. Co., Korea) was used. The epoxide equivalent weight (EEW) was 184 g/eq~190 g/eq, and the viscosity was 11,500 cps~13,500 cps at 25°C. The curing agent was 3- or 4-methyl-1,2,3,6-tetrahydrophthalic anhydride (Me-THPA), with the trade name of HN-2200 (Hitachi Chem. Co.). This curing agent is widely used in the field of electrical insulating materials. Benzyl-dimethyl amine (BDMA) as a tertiary amine was used as an accelerator (Kukdo Chem. Co. Korea). 1,1,1,3,3,3-Hexamethyl disilazane (HMDS, ACROS Organics, Fisher Scientific Inc.) was used to modify the hydrophilic surface of a fumed nanosilica (trade name: AEROSIL®300, EVONIK Industries AG) to be hydrophobic. The specific surface area of the fumed nanosilica was 270 $m^2$/g-300 $m^2$/g, and the average particle size was 12 nm. Surface-modified nanosilica was dried at 110°C for 24 h in a vacuum oven before use. The chemical structures of all materials are shown in Figure 1.

*2.2. Surface Modification of Nanosilica.* To modify the surface of fumed nanosilica with the alkyl group, it was treated with HMDS. Untreated fumed nanosilica (10 g) was dispersed in HMDS (18 g)/ethyl alcohol (160 g) solution. Ultrasonic energy (26.4 kHz, 800 W) was applied to the solution at room temperature for 1 h to remove the air layer on the fumed nanosilica surface and to wet the surface with HMDS solution simultaneously. Distilled water (290 g)/hydrochloric acid (13.3 g) solution was added to the mixture and maintained at 70°C for 5 h under the same ultrasonic condition. In this step, one HMDS molecule decomposed, producing two trimethylsilanols (Si-OH), and the produced silanols then reacted with the silanol group of the nanosilica surface producing alkyl (trimethyl group)-modified nanosilica. After the completion of the reaction, the alkyl-modified nanosilica is washed 5 times with ethanol/distilled water (40/60 wt%) mixture, dried at 110°C for 24 h in a vacuum oven, and stored in a desiccator.

*2.3. Preparation of Epoxy Nanocomposite.* Epoxy/nanosilica nanocomposites were prepared through the following procedure. Epoxy base resin (DGEBA, 100 g) and alkyl-modified nanosilica (0 g, 1 g, 3 g, 5 g, or 7 g) were well mixed at 300 rpm for 60 min using a high-speed agitator, and then, a 750 W probe-type ultrasonic processor (VC 505, Sonics & Materials Inc.) was applied to the DGEBA/nanosilica mixture at a frequency of 20 kHz for 60 min. Finally, the DGEBA/nanosilica mixture, Me-THPA (80 g), and BDMA (0.9 g) were poured into a planetary mixer and mixed for 30 min at 30°C under vacuum conditions. The final mixture was poured into a mold and cured under the following curing conditions in terms of temperature and time: 80°C × 4 h + 100°C × 3 h + 120°C × 5 h + 140°C × 5 h. In each step, temperature was raised at a rate of 1°C/min, and after curing reaction, it was slowly cooled at a rate of -1°C/min until room temperature was reached to avoid internal stress.

*2.4. Long-Term HVAC Test.* To prepare a specimen for a high voltage alternating current (HVAC) treeing test, epoxy/nanosilica mixture was poured into a mold having a cavity of 20 × 7 $mm^2$ and a height of 20 mm, in which a needle electrode was arranged beforehand to make the distance between the tip of needle electrode and the plate electrode 3.8 mm, as shown in Figure 2. A needle-type steel electrode was obtained from Ogura Jewelry Co., Japan. Its diameter and length were 1 mm and 60 mm, respectively, while its tip angle was 30° and its curvature radius was 5 $\mu$m. The epoxy mixture was cured according to the programmed curing conditions described in

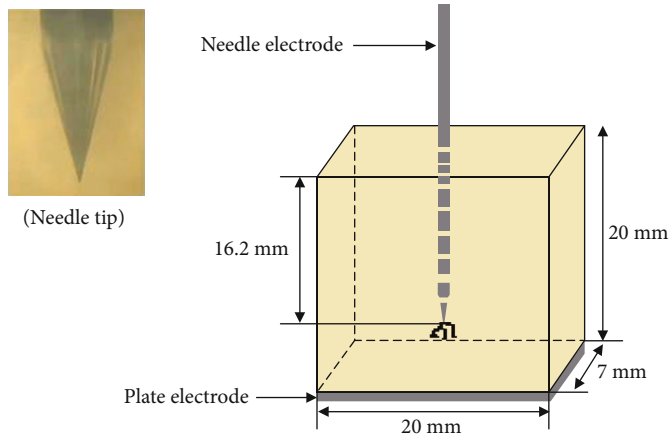


Figure 2: Arrangement of needle-plate electrodes for treeing test.

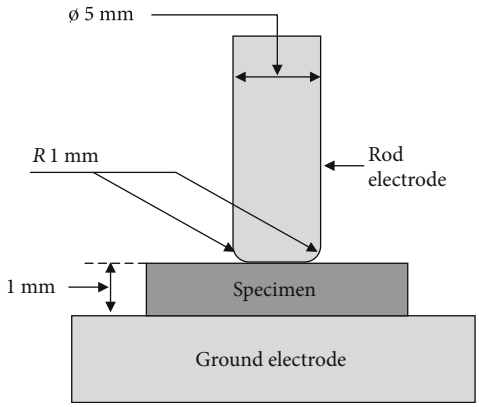


Figure 3: Arrangement of rod-ground electrodes for PD test.

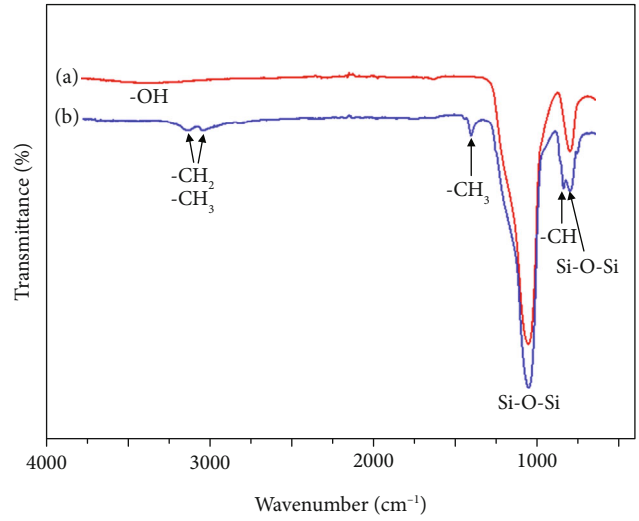


Figure 4: FT-IR spectra for (a) unmodified and (b) alkyl-modified nanosilicas.

Section 2.3. Finally, the bottom of the specimen was coated with a conductive silver paste.

To carry out a long-term HVAC breakdown test, the specimen was dipped into a 30°C insulating oil bath for 2 h, and then, a 15 kV (1 kHz) AC electric field was applied to the specimen. AC voltage was increased from 0 kV to 15 kV at a rate of 0.5 kV/s, after which it was maintained at 15 kV until breakdown occurred. Treeing shape was monitored by a stereo microscope system (S645T, EZscope) coupled with a digital camera (TOUPCAM, LCMOS05100KPA). Tree images were collected every 1 min. HVAC was generated by the AC Endurance Voltage Tester (Haefely, Germany).

*2.5. Partial Discharge Resistance Test.* As illustrated in Figure 3 for the PD resistance test, a 50 $mm^2$ specimen that was 1 mm thick was positioned on the ground electrode, and then, the rod electrode was placed on the specimen surface without any gap. The two electrodes were made of copper. If 5 kV AC with a frequency of 720 Hz was applied to the specimen for 96 h, PD occurred in the air gap portion due to the radius of curvature of the rod electrode. To measure the erosion morphology and the erosion depth due to the PD, a laser surface profiler (Dektak 150, Bruker Co.) was used. The measuring range was $14 \times 14\,mm^2$, and the resolution was 0.389 $\mu$m.

## 3. Results and Discussion

To confirm the surface modification of nanosilica, FT-IR analyses were carried out for (a) unmodified and (b) alkyl-modified nanosilicas, and the spectra are shown in Figure 4. IR characteristic peaks for unmodified nanosilica are shown at 732 $cm^{-1}$ and 1,092 $cm^{-1}$ owing to Si-O-Si bond and a broad peak at 3,406 $cm^{-1}$ owing to Si-OH bond. The IR spectrum for trimethyl (alkyl)-modified nanosilica shows new peaks at 786 $cm^{-1}$, 912 $cm^{-1}$, 1,465 $cm^{-1}$, 2,943 $cm^{-1}$, and 2,966 $cm^{-1}$ for $CH_2$ and $CH_3$ bonds. These results mean that the alkyl group is bonded to the surface of the fumed nanosilica [21]. Although not shown here, it was found through thermogravimetric analysis that the weight of the alkyl group on the nanosilica surface was 3.95 wt%.

To compare the dispersion morphologies of the unmodified or alkyl-modified nanosilica particles in epoxy nanocomposites, TEM observations were carried out, and the TEM images shown in Figure 5 were obtained. Figure 5(a) is for unmodified nanosilica particles (1 phr), where the unit phr means the parts per one hundred grams of epoxy base

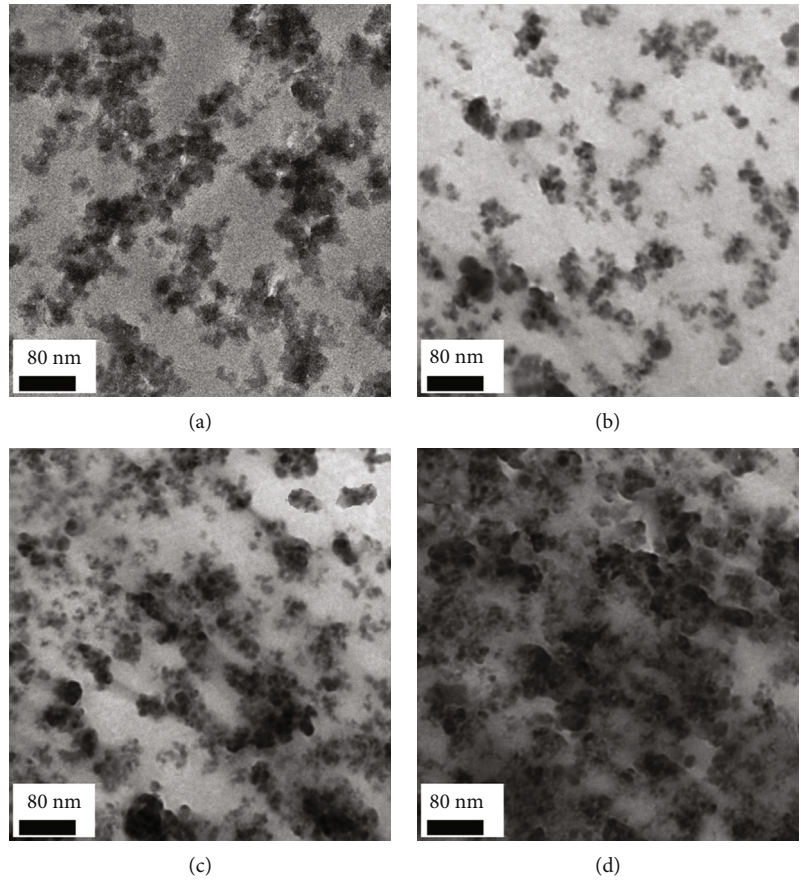


Figure 5: TEM images for nanosilica particles dispersed in epoxy nanocomposite. (a) Unmodified nanosilica content is 1 phr, and alkyl-modified nanosilica contents are (b) 1 phr, (c) 3 phr, and (d) 7 phr.

resin, and Figures 5(b)–5(d) are for alkyl-modified nanosilica particles. Alkyl-modified nanosilica contents are (b) 1 phr, (c) 3 phr, and (d) 7 phr, respectively. As shown in Figure 5(a), the unmodified nanosilica particles are not evenly dispersed in the epoxy resin, instead of forming large aggregations because their surfaces having Si-OH groups are incompatible with the hydrophobic epoxy resin. However, as shown in Figure 5(b), the modified nanosilica particles are somewhat uniformly dispersed in the epoxy nanocomposite, which is because the hydrophilic surface of the unmodified fumed nanosilica has been changed to an epoxy-friendly hydrophobic surface thanks to the alkyl group coating. These well-dispersed nanoparticles are expected to retard treeing initiation, to block treeing propagation, and to resist PD voltage. However, as the alkyl-modified nanosilica content increases, their aggregation becomes more severe. This is because the nanosilica surface area is too high compared to the epoxy weight, making the wettability of the nanosilica poor.

Figure 6 shows Weibull statistical analyses (Weibull++7.0 program of ReliaSoft (HBM Prenscia Inc.)) for HVAC electrical treeing breakdown time of epoxy nanocomposites with various contents of alkyl-modified nanosilicas. Three parameters—shape, scale, and B10 parameters—are obtained from each Weibull plot for each epoxy nanocomposite. The shape parameter is obtained from each slope, which means the data distribution. The scale parameter represents the treeing breakdown time at which there is a 63.2% cumulative probability of breakdown, which is similar in concept to the mean value of the arithmetic mean. The B10 parameter represents the treeing breakdown time at which there is a 10% cumulative probability of breakdown (90% would not break down) under the applied HVAC (15 kV, 1 kHz). When HVAC is applied to the needle tip, the electrical field generated at the needle tip can be calculated using Mason's equation as follows [22, 23]:

$$E_{\text{tip}} = \frac{2\,\text{V}}{r \cdot \ln\left(1 + 4x/r\right)} \left(\text{Mason's equation}\right), \qquad (1)$$

where $E_{\text{tip}}$ is the electrical field generated at the needle electrode tip, $V$ is applied voltage (15 kV), $r$ is needle tip radius (5 $\mu$m), and $x$ (3.8 mm) is the distance between the needle electrode tip and plate electrode. Therefore, $E_{\text{tip}}$ is 748.1 kV/mm.

All the Weibull parameters are listed in Table 1. The longest HVAC treeing breakdown time—that is to say, the longest scale parameter—is found in epoxy nanocomposite with 1 phr of alkyl-modified nanosilica, and the time is 17,412 min (12 days), which is 143.9 times longer than 121 min (2 h) for neat epoxy resin. After 1 phr of nanosilica

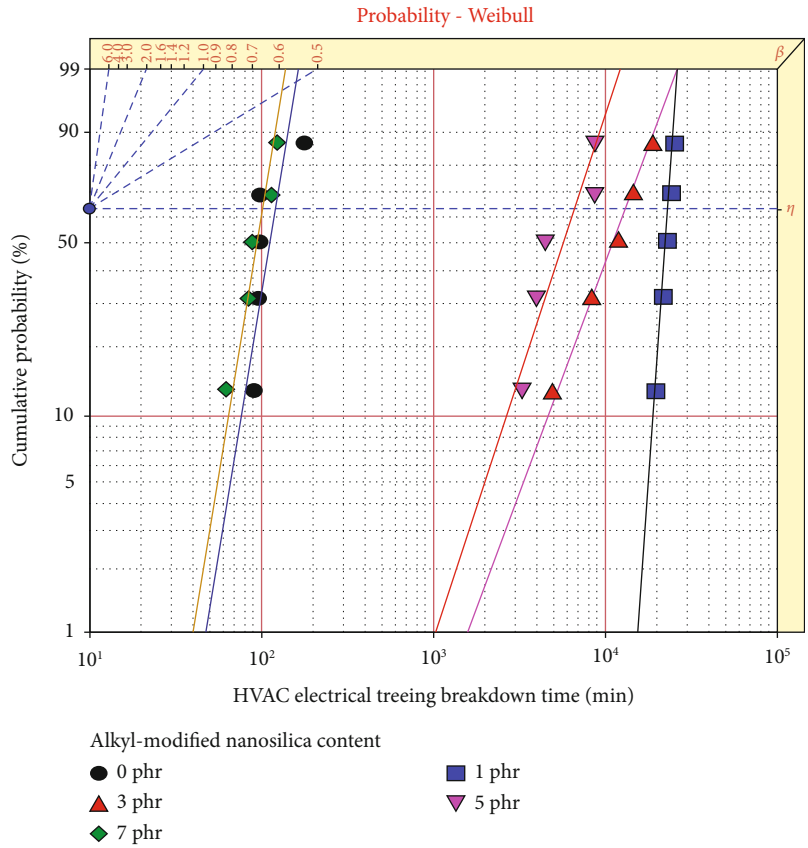


Figure 6: HVAC electrical treeing breakdown time for epoxy nanocomposites with different alkyl-modified nanosilica contents.

Table 1: Weibull parameters of HVAC treeing breakdown time for epoxy nanocomposites.

| Alkyl-modified nanosilica content | Shape parameter | Scale parameter (min) | B10 parameter (min) |
|---|---|---|---|
| 0 phr | 5.0 | 121 | 77 |
| 1 phr | 24.6 | 17,412 | 16,403 |
| 3 phr | 2.2 | 13,038 | 4,624 |
| 5 phr | 2.5 | 6,551 | 2,647 |
| 7 phr | 4.9 | 102 | 65 |

content, the scale parameter decreases as alkyl-modified nanosilica content increases. When 7 phr of alkyl-modified nanosilica is dispersed in epoxy nanocomposite, the scale parameter value becomes smaller than that of the neat epoxy resin. These results mean that evenly dispersed nanosilicas retard treeing initiation and block treeing propagation effectively; however, when nanosilica is added in excess, the beneficial effects decrease due to the aggregation of nanosilica, as shown in Figures 5(c) and 5(d).

Electrical treeing morphologies can also explain the effect of alkyl-modified nanosilica particles on the treeing propagation. In the neat epoxy system, the injected electrons from the needle tip initiate and propagate electrical treeing rapidly without any blocking, forming typical branch-type treeing as shown in Figure 7(a). On the other hand, when 1 phr of alkyl-modified nanosilica is well dispersed in the epoxy matrix, it is very difficult for injected electrons to initiate and propagate treeing, since they are blocked by the nanosilica particles. For this reason, the injected electrons find new paths, and as this process is repeated, a bush-type electrical treeing morphology is obtained, as shown in Figure 7(b). However, as 5 phr of modified nanosilica is introduced to the epoxy matrix, the blocking effect on the treeing growth rate is lowered because the modified silica nanoparticles aggregate. These results mean that the more the nanosilica is dispersed, the greater the treeing blocking effect.

Figure 8 shows the images of surface erosion morphology by PD for epoxy nanocomposites with various contents of alkyl-modified nanosilica: (a) 0 phr, (b) 1 phr, (c) 3 phr, and (d) 5 phr. In this electrode system shown in Figure 3, partial discharge occurs only near the small annular air gap at the edge of the rod electrode, so degradation does not proceed directly under the rod electrode. Thus, as shown in each image, there is a circular uneroded area. After 96 h (5 days) PD exposure, the tip edge of the electrode is discolored to black. This occurs because the epoxy molecules that are decomposed due to PD are volatilized, deposited on the electrode surface, and then carbonized by continuous discharge energy. The erosion morphologies of neat epoxy and epoxy nanocomposites have completely different patterns. The morphology of the neat epoxy system in Figure 8(a) shows severe and uneven erosions with deep and long channels at the surface of the specimen. On the other hand, in

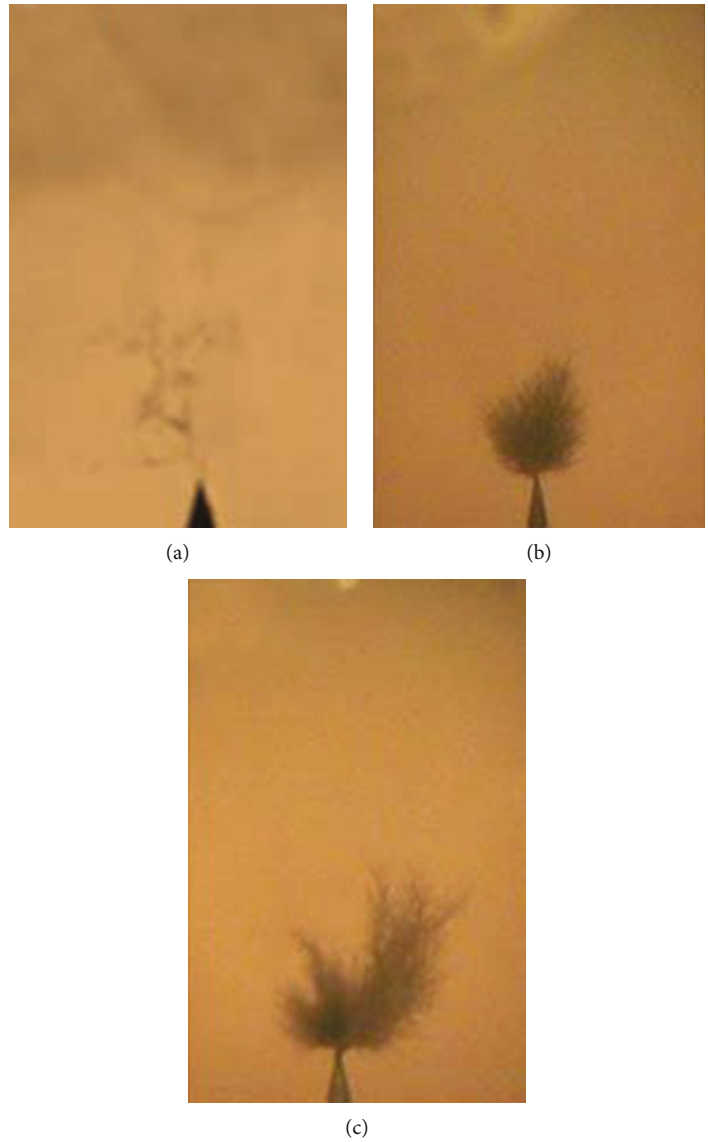

(a) (b) (c)

Figure 7: Treeing morphology in the propagation state for epoxy nanocomposites with different alkyl-modified nanosilica contents: (a) 0 phr, (b) 1 phr, and (c) 5 phr.

nanocomposites, the erosion does not progress deeply, but rather along the surface without a channel.

The surface topography for each erosion area in Figure 8 is scanned by using a surface profiler, and the erosion profile for each nanocomposite is shown in Figure 9. Alkyl-modified nanosilica contents are (a) 0 phr, (b) 1 phr, (c) 3 phr, and (d) 5 phr. In general, discharge energy emitted in the air transfers to the surface of the epoxy insulator until reaching a certain distance, but the strength gradually decreases, and therefore, the degree of degradation gradually decreases with the distance from the electrode's edge. As the PD energy continues, epoxy surface erosion proceeds, and finally, the surface is destroyed by dielectric breakdown or treeing growth [24, 25]. In the neat epoxy system, the maximum erosion depth is 378 $\mu$m, and the erosion width is 295 $\mu$m. In the nanocomposite with 1 phr of alkyl-modified nanosilica, the maximum erosion depth and the erosion width are 152 $\mu$m and 893 $\mu$m, respectively. Comparing the erosion depth, the PD resistance of the neat epoxy system is increased by 249% through the incorporation of 1 phr of alkyl-modified nanosilica. In contrast, the erosion width of the 1 phr nanocomposite is 303% wider than that of the neat epoxy system. These results mean that because well-dispersed nanosilicas block partial discharge energy in the depth direction, depth erosion is suppressed, and therefore, erosion in the surface direction occurs [26–28]. On the other hand, in the neat epoxy system without nanosilica, the PD energy is mostly used for the erosion in the depth direction, so that deep erosion occurs at the rod electrode's edge region. However, as nanosilica content increases, the depth of erosion is reduced. When 5 phr of alkyl-modified nanosilica is incorporated into the epoxy matrix, erosion hardly occurs at the edge of the rod electrode where partial discharge occurs, and there is no erosion under the rod electrode. This means that high content of the

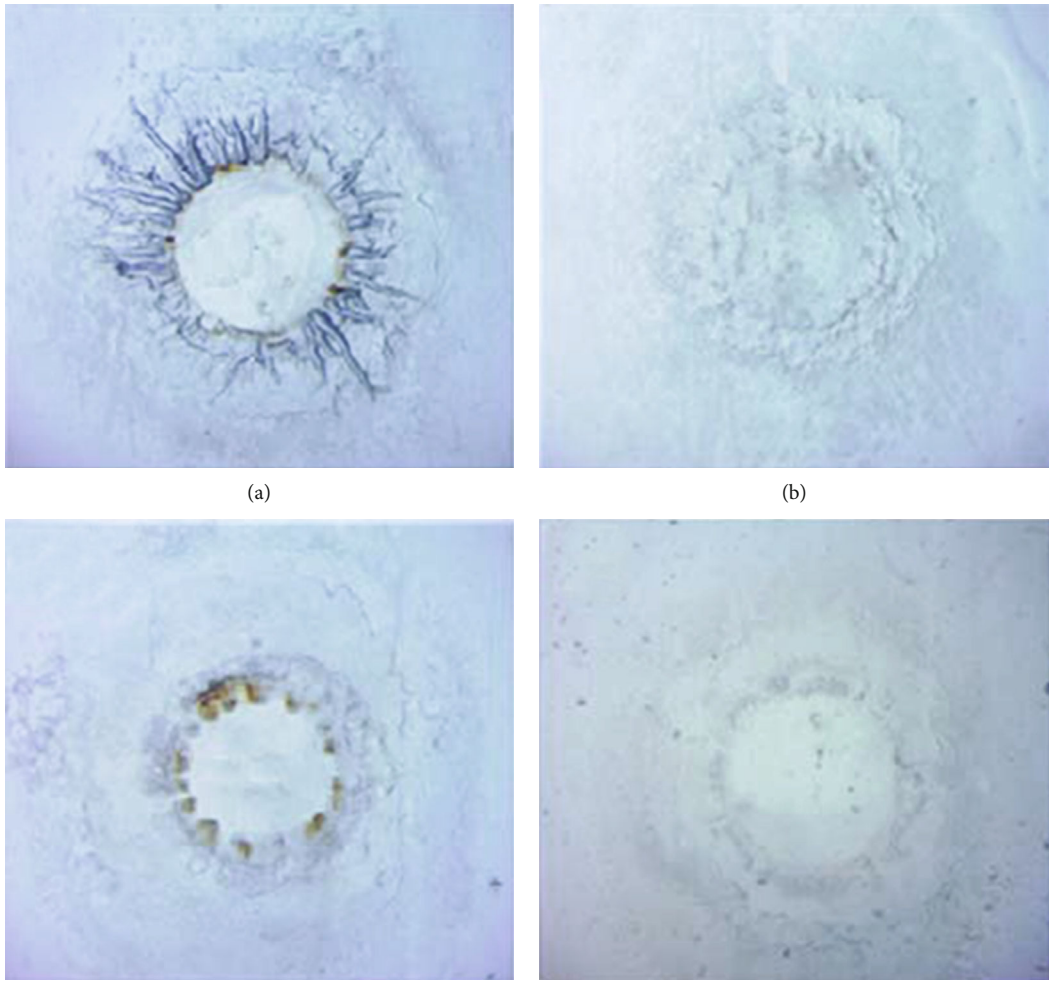


Figure 8: Surface erosion morphology by PD for epoxy nanocomposites with different alkyl-modified nanosilica contents: (a) 0 phr, (b) 1 phr, (c) 3 phr, and (d) 5 phr.

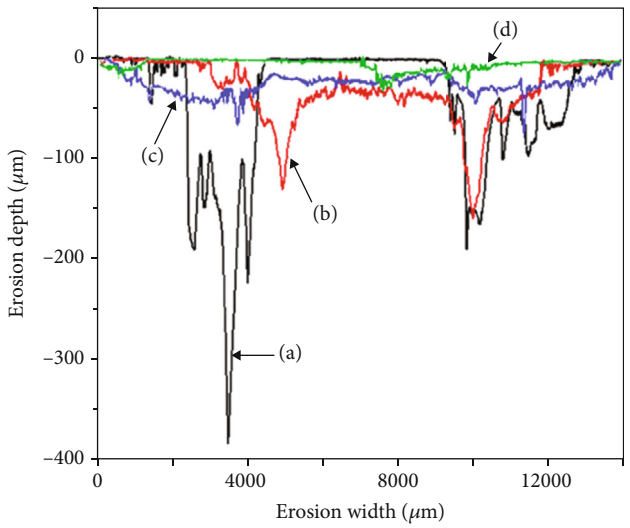


Figure 9: Surface profiles by PD for epoxy nanocomposites with different alkyl-modified nanosilica contents: (a) 0 phr, (b) 1 phr, (c) 3 phr, and (d) 5 phr.

modified nanosilica not only suppresses erosion in the depth direction but also suppresses erosion in the surface direction. PD resistance of 5 phr of the nanocomposite is 1,251% higher than that of neat epoxy. PD resistance is highest in 5 phr of the nanocomposite, while treeing resistance is highest in 1 phr of the nanocomposite. This is because PD energy is applied to a wide range of specimens, while treeing energy is concentrated at the tip of the treeing. In other words, if nanosilica content is too high, the epoxy cannot wet the surface of alkyl-modified nanosilica, so the concentrated treeing energy easily penetrates among the aggregated nanosilicas. On the other hand, it is considered that the penetration of PD energy applied to a wide range is blocked effectively.

## 4. Conclusions

The hydrophilic surface of fumed nanosilica is modified to a hydrophobic surface through treatment with a trimethyl silane coupling agent, and the modified nanosilicas are incorporated into the epoxy matrix in order to prepare an epoxy nanocomposite for electrical insulating material. The

bonding of trimethyl silane on the nanosilica surface is confirmed by the appearance of new peaks for the $CH_2$ and $CH_3$ groups through FT-IR analysis. TEM observations show that 1 phr of the alkyl-modified nanosilicas is well-dispersed in the epoxy nanocomposite; however, aggregation becomes severe as the nanosilica content increases. The longest HVAC treeing breakdown time is found in epoxy nanocomposite with 1 phr of alkyl-modified nanosilica, and the time is 17,412 min (12 days). This value is 143.9 times longer than the 121 min (2 h) HVAC treeing breakdown time of neat epoxy resin. After 1 phr of nanosilica content, treeing breakdown time decreases as alkyl-modified nanosilica content increases. These results mean that properly well-dispersed nanosilicas retard treeing initiation and block treeing propagation effectively, but as the nanosilica content increases, the blocking effect on the treeing growth rate is reduced by the aggregation of the modified silica nanoparticles. The electrical treeing morphology for a neat epoxy system has a branch type, while for epoxy nanocomposites, it has a bush type. As is well known, the treeing breakdown time of the bush type is much longer than that of the branch type due to the blocking of alkyl-modified nanosilica particles. PD resistance increases with the content of alkyl-modified nanosilica. The PD resistance of the neat epoxy system is increased by 249% and 1,251% through the incorporation of 1 phr and 5 phr of alkyl-modified nanosilica, respectively. Treeing resistance is highest in 1 phr nanocomposite, while PD resistance is highest in 5 phr of nanocomposite. As alkyl-modified nanosilica content is too high, the concentrated treeing energy easily penetrates among the aggregated nanosilicas, but PD energy is effectively blocked.

## Data Availability

There is no underlying data.

## Conflicts of Interest

The author declares that they have no conflicts of interest.

## Acknowledgments

This work was supported by Joongbu University in 2019.

## References

[1] B. Du, J. Su, M. Tian, T. Han, and J. Li, "Understanding trap effects on electrical treeing phenomena in EPDM/POSS composites," *Scientific Reports*, vol. 8, no. 1, p. 8481, 2018.

[2] M. A. Fard, M. E. Farrag, A. Reid, and F. Al-Naemi, "Electrical treeing in power cable insulation under harmonics superimposed on unfiltered HVDC voltages," *Energies*, vol. 12, no. 16, p. 3113, 2019.

[3] E. Kantar, E. Ildstad, and S. Hvidsten, "Effect of elastic modulus on the tangential AC breakdown strength of polymer interfaces," *IEEE Transactions on Dielectrics and Electrical Insulation*, vol. 26, no. 1, pp. 211–219, 2019.

[4] M. Danikas, D. Papadopoulos, and S. Morsalin, "Propagation of electrical trees under the influence of mechanical stresses: a short review," *Engineering, Technology and Applied Science Research*, vol. 9, no. 1, pp. 3750–3756, 2019.

[5] R. Sarathi, A. Nandini, and T. Tanaka, "Understanding treeing phenomena and space charge effect in gamma-irradiated XLPE cable insulation," *Electrical Engineering*, vol. 93, no. 4, pp. 199–207, 2011.

[6] Z. Cai, X. Wang, L. Li, and W. Hong, "Electrical treeing: a phase-field model," *Extreme Mechanics Letters*, vol. 28, pp. 87–95, 2019.

[7] J. J. Park and J. Y. Lee, "Effect of nano-sized layered silicate on AC electrical treeing behavior of epoxy/layered silicate nanocomposite in needle-plate electrodes," *Materials Chemistry and Physics*, vol. 141, no. 2-3, pp. 776–780, 2013.

[8] H. Zheng, S. M. Rowland, and N. Jiang, "Influence of electrode separation on electrical treeing in a glassy epoxy resin," in *in 2017 IEEE Conference on Electrical Insulation and Dielectric Phenomenon (CEIDP)*, pp. 769–772, TX, USA, 2017.

[9] H. Zheng, S. M. Rowland, I. Iddrissu, and Z. Lv, "Electrical treeing and reverse tree growth in an epoxy resin," *IEEE Transactions on Dielectrics and Electrical Insulation*, vol. 24, no. 6, pp. 3966–3973, 2017.

[10] Y. S. Cho, M. J. Shim, and S. W. Kim, "Characteristics of polymer insulator materials: voltage-lifetime characteristics of DGEBA/MDA/SN system," *Materials Chemistry and Physics*, vol. 66, no. 1, pp. 70–76, 2000.

[11] R. Sarathi, R. K. Sahu, and P. Rajeshkumar, "Understanding the thermal, mechanical and electrical properties of epoxy nanocomposites," *Materials Science and Engineering: A*, vol. 445–446, pp. 567–578, 2007.

[12] M. Bell, T. Krentz, J. K. Nelson et al., "Investigation of dielectric breakdown in silica-epoxy nanocomposites using designed interfaces," *Journal of Colloid and Interface Science*, vol. 495, pp. 130–139, 2017.

[13] X. Wang, Y. Zhao, K. Yang, S. Zhang, and Y. He, "Effect of silane coupling agent modified alumina filler on breakdown characteristics of epoxy composites," in *in 2018 IEEE 2nd International Electrical and Energy Conference (CIEEC)*, pp. 544–547, Beijing, China, 2018.

[14] H. Nguyen, A. Y. Mirza, W. Chen et al., "Discharge resistant epoxy/clay nanocomposite for high torque density electrical propulsion," in *in 2018 IEEE Conference on Electrical Insulation and Dielectric Phenomena (CEIDP)*, pp. 171–174, Cancun, Mexico, 2018.

[15] T. Onishi, S. Hashimoto, M. Tomita et al., "Nano-scale evaluation of electrical tree initiation in silica/epoxy nanocomposite thin film," in *in 2017 international symposium on electrical insulating materials (ISEIM)*, vol. 1, pp. 359–362, Toyohashi, Japan, 2017.

[16] Z. Li, G. Sheng, X. Jiang, and T. Tanaka, "Effects of inorganic fillers on withstanding short-time breakdown and long-time electrical aging of epoxy composites," *IEEJ Transactions on Electrical and Electronic Engineering*, vol. 12, no. S2, pp. S10–S15, 2017.

[17] H. Li, C. Wang, Z. Guo et al., "Effects of silane coupling agents on the electrical properties of silica/epoxy nanocomposites," in *in 2016 IEEE International Conference on Dielectrics (ICD)*, pp. 1036–1039, Montpellier, France, 2016.

[18] X. Lyu, H. Wang, Z. Guo, and Z. Peng, "Dielectric properties of epoxy-Al2O3 nanocomposites," in *in 2016 IEEE International Conference on Dielectrics (ICD)*, pp. 1081–1084, Montpellier, France, 2016.

[19] J. J. Park, "Effect of electric frequency on the partial discharge resistance of epoxy systems with two diluents," *Transactions on Electrical and Electronic Materials*, vol. 14, no. 6, pp. 317–320, 2013.

[20] N. Müller, S. Lang, and R. Moos, "Influence of ambient conditions on electrical partial discharge resistance of epoxy anhydride based polymers using IEC 60343 method," *IEEE Transactions on Dielectrics and Electrical Insulation*, vol. 26, no. 5, pp. 1463–1470, 2019.

[21] A. R. Kim, M. Vinothkannan, and D. J. Yoo, "Artificially designed, low humidifying organic–inorganic (SFBC-50/FSiO2) composite membrane for electrolyte applications of fuel cells," *Composites Part B: Engineering*, vol. 130, pp. 103–118, 2017.

[22] J. H. Mason, "Breakdown of solid dielectrics in divergent fields," *in Proceedings of the IEE - Part B: Radio and Electronic Engineering*, vol. 102, no. 2, pp. 725–727, 1955.

[23] B. Du, M. Tian, J. Su, and T. Han, "Electrical tree growth characteristics in epoxy resin with harmonic superimposed DC voltage," *IEEE Access*, vol. 7, pp. 47273–47281, 2019.

[24] C. H. Lee and J. J. Park, "The partial discharge resistances of epoxy-nano-and-micro composites," *Transactions on Electrical and Electronic Materials*, vol. 11, no. 2, pp. 89–91, 2010.

[25] Z. Lv, S. M. Rowland, S. Chen, H. Zheng, and I. Iddrissu, "Evolution of partial discharges during early tree propagation in epoxy resin," *IEEE Transactions on Dielectrics and Electrical Insulation*, vol. 24, no. 5, pp. 2995–3003, 2017.

[26] G. Suriati, M. Mariatti, and A. Azizan, "Effects of filler shape and size on the properties of silver filled epoxy composite for electronic applications," *Journal of Materials Science: Materials in Electronics*, vol. 22, no. 1, pp. 56–63, 2011.

[27] P. Preetha and M. J. Thomas, "Partial discharge resistant characteristics of epoxy nanocomposites," *IEEE Transactions on Dielectrics and Electrical Insulation*, vol. 18, no. 1, pp. 264–274, 2011.

[28] T. Tanaka and T. Iizuka, "Generic PD resistance characteristics of polymer nanocomposites," in *in 2010 Annual Report Conference on Electrical Insulation and Dielectric Phenomena (CEIDP)*, pp. 17–20, IN, USA, 2010.